

New polytypes of long-period stacking ordered structures in a near-equilibrium $Mg_{97}Zn_1Y_2$ alloy

Q. Q. Jin, X. H. Shao, X. B. Hu, Z. Z. Peng & X. L. Ma

To cite this article: Q. Q. Jin, X. H. Shao, X. B. Hu, Z. Z. Peng & X. L. Ma (2017) New polytypes of long-period stacking ordered structures in a near-equilibrium $Mg_{97}Zn_1Y_2$ alloy, Philosophical Magazine Letters, 97:5, 180-187, DOI: [10.1080/09500839.2017.1311426](https://doi.org/10.1080/09500839.2017.1311426)

To link to this article: <https://doi.org/10.1080/09500839.2017.1311426>



Published online: 03 Apr 2017.



Submit your article to this journal [↗](#)



Article views: 87



View related articles [↗](#)



View Crossmark data [↗](#)



New polytypes of long-period stacking ordered structures in a near-equilibrium $\text{Mg}_{97}\text{Zn}_1\text{Y}_2$ alloy

Q. Q. Jin^{a,b}, X. H. Shao^b, X. B. Hu^{b†}, Z. Z. Peng^b and X. L. Ma^{b,c}

^aSchool of Materials Science and Engineering, University of Science and Technology of China, Hefei, China; ^bShenyang National Laboratory for Materials Science, Institute of Metal Research, Chinese Academy of Sciences, Shenyang, China; ^cSchool of Materials Science and Engineering, Lanzhou University of Technology, Lanzhou, China

ABSTRACT

By atomic-scale high-angle annular dark-field scanning transmission electron microscopy, the long-period stacking ordered (LPSO) structures in a near-equilibrium $\text{Mg}_{97}\text{Zn}_1\text{Y}_2$ (at.%) alloy have been characterised. In addition to 18R and 14H, new polytypes of LPSO structures are analysed and determined as 60R, 78R, 26H, 96R, 38H, 40H, 108H and 246R. All of these LPSO structures feature AB'C'A building blocks with two Mg layers and three Mg layers sandwiched between them. The Bravais lattices and space groups of new polytypes of LPSO structures were easily determined via the newly introduced method. A structural relationship between the LPSOs is proposed.

ARTICLE HISTORY

Received 15 December 2016
Accepted 9 March 2017

KEYWORDS

Magnesium alloys; long-period stacking ordered (LPSO) structure; scanning transmission electron microscopy; electron diffraction

Mg–M–RE (M=Al, Co, Ni, Cu and Zn; RE=Y, Gd, Dy, Ho, Er and Tb) based systems have received considerable attention over the past decade, on account of their excellent mechanical properties [1–6] and unique structural characteristics [7–14]. For example, $\text{Mg}_{97}\text{Zn}_1\text{Y}_2$ alloys fabricated by a rapid solidification powder metallurgy process realised tensile yield strength exceeding 600 MPa with an elongation of 5% at room temperature [1,2]. Subsequently, various as-cast $\text{Mg}_{97}\text{M}_1\text{RE}_2$ (M=Zn, Ni and Cu; RE = rare earth) alloys are reported to exhibit tensile yield strength in the range of 297–377 MPa after conventional hot extrusion process [3–5]. Long-period stacking ordered (LPSO) structures are believed to play essential roles in improving mechanical properties of these Mg alloys [6]. In order to understand the inherent relationship between the structures, formation mechanism and mechanical properties, great effort has been devoted to investigate the atomic structures of the LPSO phases [8,10,12,15–20] and exploring new polytypes in various systems [11,13,14,21]. 10H, 18R, 14H and 24R LPSO structures containing AB'C'A building blocks sandwiching one, two, three and four Mg layers were observed in Mg–Zn–RE alloys [7,13,22], where B' and C' layers are enriched with Zn/RE atoms. Whilst in Mg–Co–Y alloys, 15R, 12H and 21R LPSO structures feature AB'C building blocks sandwiching two, three and four Mg layers, respectively [11,13]. Recently, we detected six polytypes containing both

CONTACT X. H. Shao  xhshao@imr.ac.cn

[†]Current Address: Nanostructures Research Laboratory, Japan Fine Ceramics Center, Nagoya 456-8587, Japan

Table 1. Translation and point symmetry of various components made up into LPSO structures in Mg–M–RE alloys.

Component	Translation	Component	Translation	Component	Point symmetry
F(2k)	s_3	T(2k)	s_2	F-block	$\bar{1}$
$\bar{F}(2k)$	s_2	$\bar{T}(2k)$	s_3	T-block	$\bar{1}$
F(2k + 1)	s_1	T(2k + 1)	s_3	(2k)-Mg	$\bar{1}$
$\bar{F}(2k + 1)$	s_1	$\bar{T}(2k + 1)$	s_2	(2k + 1)-Mg	m

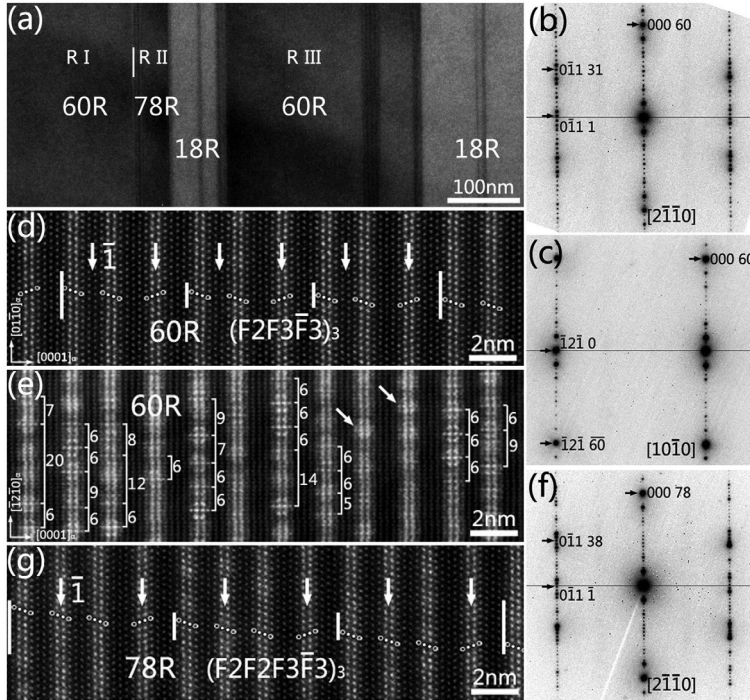


Figure 1. (a) Low-magnification TEM image showing the coexistence of 18R, 60R and 78R structures in the near-equilibrium $\text{Mg}_{97}\text{Zn}_1\text{Y}_2$ as-cast alloy. SAED patterns of the 60R structure obtained along the (b) $[2\bar{1}\bar{1}]_a$ and (c) $[1\ 0\ \bar{1}]_a$ zone axis. Atomic-resolution HAADF-STEM images of 60R structure viewed along the (d) $[2\bar{1}\bar{1}]_a$ and (e) $[1\ 0\ \bar{1}]_a$ zone axis, where the distance between neighbouring $\text{Zn}_6\text{Y}_8\text{X}(\text{Mg}, \text{Zn}, \text{Y})$ clusters are highlighted. (f) SAED pattern of the 78R structure obtained along $[2\bar{1}\bar{1}]_a$ direction. (g) Atomic-resolution HAADF-STEM image of 78R structure viewed along $[2\bar{1}\bar{1}]_a$ zone axis.

AB'C'A and AB'C building blocks, such as 72R and 60H, in an $\text{Mg}_{92}\text{Co}_2\text{Y}_6$ alloy [13], and an ultra-long 654R structure formed via ordered intergrowth of 15R and 12H in an $\text{Mg}_{88}\text{Co}_5\text{Y}_7$ alloy [14]. In view of the existence of various LPSO structures in Mg–Co–Y alloy, we expect that there are also new types of LPSO structures in $\text{Mg}_{97}\text{Zn}_1\text{Y}_2$ alloys.

In this work, we unravelled the crystallography of eight new polytypes of LPSO structures in a near-equilibrium $\text{Mg}_{97}\text{Zn}_1\text{Y}_2$ alloy by a combination of transmission electron microscopy (TEM) and scanning transmission electron microscopy (STEM) microscopy. Each polytype, 60R, 78R, 26H, 96R, 38H, 40H, 108H and 246R, is composed of AB'C'A building blocks, two and three Mg layers. We further determined their crystallography via our method and here propose their structural relationship.

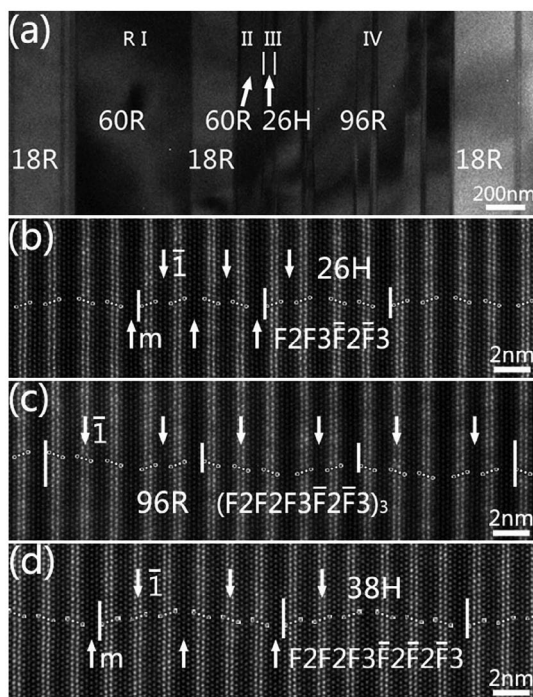


Figure 2. (a) Low-magnification TEM image showing 18R, 60R, 26H and 96R structures coexisting in the $\text{Mg}_{97}\text{Zn}_1\text{Y}_2$ alloy. Atomic-resolution HAADF-STEM images of (b) 26H, (c) 96R and (d) 38H structures viewed along $[2\bar{1}\bar{1}]_a$ zone axis.

A ternary alloy with nominal composition Mg–1.0at.% Zn–2.0at.% Y was prepared by melting high-purity Mg, Zn and Mg–30 wt.% Y master ingots, and then cooling the melt down to the room temperature at the rate of 4 K/min in a resistance furnace under a protective mixed gas of SF_6 (0.5 vol.%) and CO_2 (99.5 vol.%). Foils for TEM and high-angle annular dark-field scanning transmission electron microscopy (HAADF-STEM) observations were prepared using standard TEM sample preparation methods. New LPSO structures were detected by bright-field (BF) imaging and selected-area electron diffraction (SAED), using a Tecnai G² F30 equipped with a field emission gun and operated at 300 kV. Atomic-resolution HAADF-STEM imaging was then performed with an aberration-corrected Titan³™ G² 60–300 operated at 300 kV, equipped with a high-brightness field emission gun (X-FEG) and double Cs correctors from CEOS.

We introduce new methods to easily determine the Bravais lattices and space groups of LPSO structures in Mg–M–RE alloys based on their expressions by our presented notations in previous work [13]. In Mg–M–RE alloys, $AB'C'A$ (and/or $AC'B'A$) building blocks are defined as F-blocks and denoted as F (and/or \bar{F}); whilst $AB'C$ (and/or $AC'B$) building blocks are defined as T-block and denoted as T (and/or \bar{T}). The n ($n = \text{integer}$) means the number of Mg layers sandwiched between the F- and/or T-blocks, written as $n\text{-Mg}$. The subscript number refers the number of repeated (sub) unit cells. Now, we introduce the translations of the LPSO structure's components. The relation between the first layer of a structure and the layer following the structure is one of the three translations, $\mathbf{s}_1 = \mathbf{e}$, $\mathbf{s}_2 = \frac{2}{3}\mathbf{a} + \frac{1}{3}\mathbf{b} + \mathbf{e}$ and $\mathbf{s}_3 = \frac{1}{3}\mathbf{a} + \frac{2}{3}\mathbf{b} + \mathbf{e}$, where \mathbf{a} and \mathbf{b} denote hexagonal basic translational vectors within

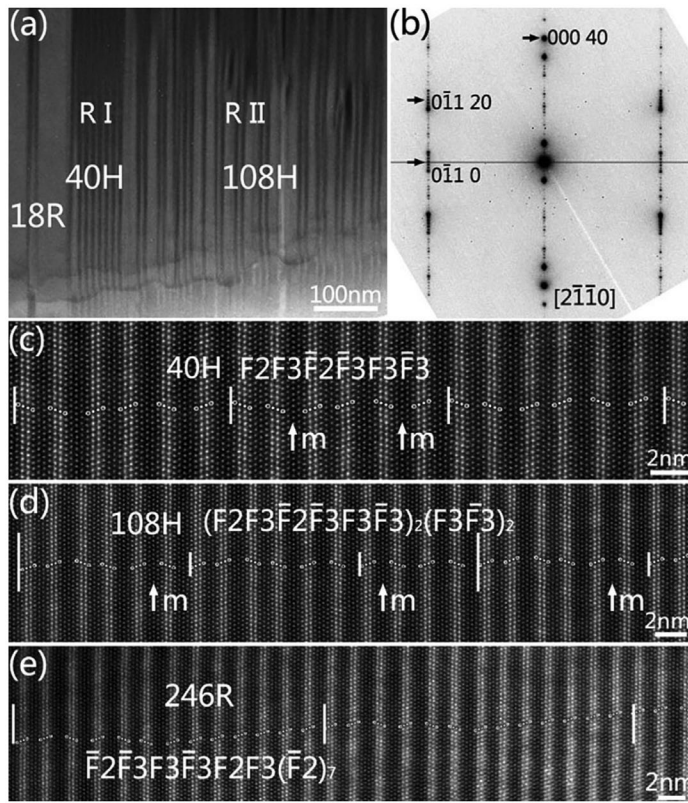


Figure 3. (a) Low-magnification TEM image showing the coexistence of 18R, 40H and 108H LPSO structures in the $\text{Mg}_{97}\text{Zn}_1\text{Y}_2$ alloy. (b) SAED pattern of 40H obtained along $[2\bar{1}\bar{1}]_a$ zone axis. Atomic-resolution HAADF-STEM images of (c) 40H, (d) 108H and (e) 246R viewed along $[2\bar{1}\bar{1}]_a$ zone axis.

Table 2. Expressions and crystallographic parameters of new LPSO structures in this $\text{Mg}_{97}\text{Zn}_1\text{Y}_2$ alloys.

LPSO	Expressions	c (nm)	Space groups
60R	$(\text{F}2\text{F}3\bar{\text{F}}3)_3$	15.6	$R\bar{3}m$
78R	$(\text{F}2\text{F}2\text{F}3\bar{\text{F}}3)_3$	20.3	$R\bar{3}m$
26H	$\text{F}2\text{F}3\bar{\text{F}}2\bar{\text{F}}3$	6.77	$P6_3/mmc$
38H	$\text{F}2\text{F}2\text{F}3\bar{\text{F}}2\bar{\text{F}}2\bar{\text{F}}3$	9.90	$P6_3/mmc$
96R	$(\text{F}2\text{F}2\text{F}3\bar{\text{F}}2\bar{\text{F}}3)_3$	25.0	$R\bar{3}m$
40H	$\text{F}2\text{F}3\bar{\text{F}}2\bar{\text{F}}3\text{F}3\bar{\text{F}}3$	10.4	$P\bar{6}m2$
108H	$(\text{F}2\text{F}3\bar{\text{F}}2\bar{\text{F}}3\text{F}3\bar{\text{F}}3)_2(\text{F}3\bar{\text{F}}3)_2$	27.1	$P\bar{6}m2$
246R	$[\text{F}2\text{F}3\bar{\text{F}}2\bar{\text{F}}3\text{F}3\bar{\text{F}}3(\text{F}2)]_3$	64.1	$R\bar{3}m$

the layer, and \mathbf{e} is a vector perpendicular to \mathbf{a} and \mathbf{b} . The translation of $\text{F}(2k)$ ($k = \text{integer}$) structure with stacking sequence of $\overline{\text{AB}'\text{C}'\text{A}}$ $(\text{CA})_k$ $(\text{C} \dots)$ is \mathbf{s}_3 , whilst the rest are listed in Table 1. The unit cell's translation of an LPSO structure is \mathbf{s}_1 . The translation of a repeated unit is the sum of all the structural components' translations. The Bravais lattice type of LPSO structures with repeated unit possessing translation of \mathbf{s}_1 , \mathbf{s}_2 and \mathbf{s}_3 are correspondingly hexagonal, positive rhombohedral structure and anti-rhombohedral structure, respectively.

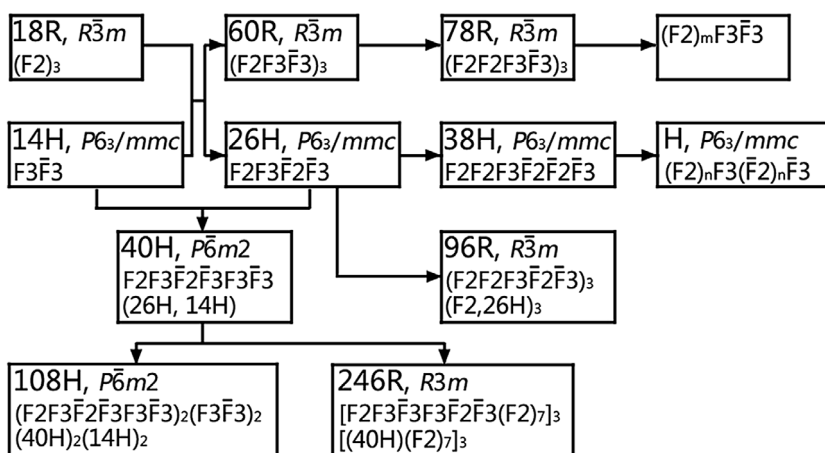


Figure 4. (a) The schematic diagram of structure relationship between LPSO structures in this $\text{Mg}_{97}\text{Zn}_1\text{Y}_2$ alloy.

In addition, the symmetry of LPSO structures can be also deduced based on their expressions by new notations. The components, F-block, T-block and $(2k)$ -Mg, possess an inversion centre, whilst the component $(2k + 1)$ -Mg possesses a mirror at the centre of them, as listed in Table 1. The point symmetry of LPSO structures is in accordance with the components. For example, the 60R structure, $\text{F2F3}\overline{\text{F3}}\text{F2F3}\overline{\text{F3}}\text{F2F3}\overline{\text{F3}}$, shows the components at the locations of the equidistant from 2-Mg or $\overline{\text{F}}$ -block in bold are absolutely the same, and building blocks shear in same directions, which implies that the existence of inversion centres at the centre of them. The 40H structure, $\text{F2F3}\overline{\text{F2}}\overline{\text{F3}}\text{F3}\overline{\text{F3}}$, shows the components at the locations of the equidistant from 3-Mg in bold are same, but building blocks shear in opposite directions, which indicates that there are mirrors at the centre of 3-Mg. Up to now, no LPSO structure with a space group of $P6_3mc$ and 2_1 screw zone axis has been observed in Mg–M–RE alloys. Thus, a conceived $\text{F2T3}\overline{\text{F2}}\overline{\text{T3}}$ structure is present here. Obviously, the two parts of the structure are the same but building blocks shear in opposite direction, indicating there is a 2_1 screw zone axis along the stacking direction. The corresponding space groups of LPSO structures can be deduced based on their special symmetry [13].

New polytypes of LPSO structures, in addition to the dominate 18R and 14H LPSO structures, were detected in the as-cast $\text{Mg}_{97}\text{Zn}_1\text{Y}_2$ alloy. New LPSO structures in R I (Region I) to R III coexisting with 18R are shown in Figure 1(a). Figure 1(b)–(c) display the SAED patterns of the LPSO structure in R I, taken from $[2\bar{1}\bar{1}0]_{\text{Mg}}$ and $[10\bar{1}0]_{\text{Mg}}$ zone axis, respectively. There are 19 extra diffraction spots spaced equally between the central spot and $(0002)_{\text{Mg}}$ spot, which can be indexed as either 20H or 60R in hexagonal coordinates. However, the $(0\bar{1}10)$ spot does not appear (Figure 1b), whilst the $(\bar{1}2\bar{1}0)$ spot does appear (Figure 1c), indicating that it can be determined as 60R with rhombohedral lattice type based on the analysis of SAED patterns of LPSO structures. Its lattice parameters are estimated as $a = 0.321$ nm and $c = 15.6$ nm in hexagonal coordinate by assuming $a_{60\text{R}} = a_{\text{Mg}}$ and $c_{60\text{R}} = \frac{1}{2}60c_{\text{Mg}}$. The sharp reflection spots in the SAED patterns and no detectable streak at $1/2(0\bar{1}\bar{1}l)$ and $n/6(\bar{1}2\bar{1}l)$ reciprocal lattice rows in Figure 1(b)–(c), suggest that the present LPSO phase is a stacking ordered and in-plane chemical disordered structure [8,11–13,16].

The atomic-resolution HAADF-STEM image of the 60R structure is shown in Figure 1(d), viewed along $[2\bar{1}\bar{1}0]_{\alpha}$ zone axis. Apparently, the repeated structure is $F2F3\bar{F}3$ with a translation of s_3 . Thus, it is 60R structure and expressed as $(F2F3\bar{F}3)_3$. Its space group can be determined as $R\bar{3}m$, as inversion centres exist in the components denoted by arrows in Figure 1(d). The atomic-resolution HAADF-STEM image of 60R structure viewed along $[10\bar{1}0]_{\alpha}$ zone axis in a thin area of the specimen is presented in Figure 1(e). The Zn_6Y_8X ($X=Mg, Zn, Y$) clusters [8,9,12,18,20] in the F-blocks of 60R structure can be detected, and the distances between neighbour clusters are marked in the image. Some clusters arrange locally ordered with a distance of six times $d_{1\bar{2}10}$ (0.160 nm), indicating they distribute in $2\sqrt{3}a_{Mg} \times 2\sqrt{3}a_{Mg}$ two-dimensional unit cells [8,10,12,20]. Some clusters arranged disorderedly with random distances, or no clusters can be distinguished in some other areas. Thus, the clusters are disordered or locally ordered in the basal planes, agreeing well with the results of SAED pattern (Figure 1b–c).

Figure 1(f) is an SAED pattern of the structure in R II along $[2\bar{1}\bar{1}0]_{Mg}$ direction, in which extra diffraction spots appear at positions $n/26$ $(0002)_{Mg}$ (n is an integer) and $(0\bar{1}10)$ spot disappears, clarifying that it is 78R structure [13] with lattice parameters $a_{78R} = a_{Mg} = 0.321$ nm and $c_{78R} = \frac{1}{2} \times 78 \times c_{Mg} = 20.3$ nm in hexagonal coordinate. Figure 1(g) shows atomic-resolution HAADF-STEM image of the 78R structure along $[2\bar{1}\bar{1}0]_{\alpha}$ zone axis. The repeated structure can be expressed as $F2F2F3\bar{F}3$ with translation of s_2 , indicating it is a rhombohedral lattice and can be expressed as $(F2F2F3\bar{F}3)_3$. Its repeat unit, $F2F2F3\bar{F}3$, shows inversion centres in the F-blocks in bold, suggesting its space group is $R\bar{3}m$.

Figure 2(a) is another low-magnification TEM image of $Mg_{97}Zn_1Y_2$ alloy, where new LPSO structures in R I to R IV in dark contrast. The LPSO structures in R I and R II were proved to be 60R. The zoom-in HAADF-STEM image shown in Figure 2(b) demonstrates that the repeated structure in R III can be expressed as $F2F3\bar{F}2\bar{F}3$ with translation of s_1 , indicating 26H structure. The expression, $F2F3\bar{F}2\bar{F}3$, implies the existence of mirrors at the centre of 3-Mg structure in bold. Meanwhile, $F2F3\bar{F}2\bar{F}3$ also indicates inversion centres at the centre of 2-Mg structure. Thus, the space group of 26H structure is $P6_3/mmc$. The atomic resolution HAADF-STEM image in Figure 2(c) exhibits the repeated structure in R IV is $F2F2F3\bar{F}2\bar{F}3$ or $(F2, 26H)$ with translation of s_3 , indicating 96R structure with stacking sequence of $(F2F2F3\bar{F}2\bar{F}3)_3$. The expression, $F2F2F3\bar{F}2\bar{F}3$, indicates inversion centres at the centre of 2-Mg and F-blocks in bold. Thus, the space group of 96R is $R\bar{3}m$. In addition, Fig. 2(d) presents another LPSO structure with repeated structure $F2F2F3\bar{F}2\bar{F}2\bar{F}3$ and a translation of s_1 , indicates 38H structure. There are mirrors at the centre of 3-Mg structure and inversion centres at the centre of F-blocks in bold, so its space group is $P6_3/mmc$.

The coexistence of 18R and two other types of superstructures were shown in Figure 3(a). Figure 3(b) shows the SAED pattern of the superstructure in R I, recorded along $[2\bar{1}\bar{1}0]_{Mg}$ zone axis. The extra diffraction spots in the SAED pattern appear at positions $n/40$ $(0002)_{Mg}$ (n is an integer), combining the appearance of $(0\bar{1}10)$ spot, proving that it is 40H structure. Figure 3(c) presents an atomic-scale HAADF-STEM image of 40H with repeated structure $F2F3\bar{F}2\bar{F}3F3\bar{F}3$, which can also be denoted as $(26H, 14H)$ with translation of s_1 . Its expression, $F2F3\bar{F}2\bar{F}3F3\bar{F}3$, shows mirrors at the centre of 3-Mg in bold, suggesting its space group is $P\bar{6}m2$. The repeated structure in Figure 3(d) is $(F2F3\bar{F}2\bar{F}3F3\bar{F}3)_2(F3\bar{F}3)_2$ and can be marked as $(40H)_2(14H)_2$ with translation of s_1 , indicating the superstructure is 108H structure. Similarly, mirrors can be marked at the centre of 3-Mg in bold if it was noted as $F2F3\bar{F}2\bar{F}3F3\bar{F}3F2F3\bar{F}2\bar{F}3F3\bar{F}3F3\bar{F}3F3\bar{F}3F3\bar{F}3$, indicating its space group is $P\bar{6}m2$. Besides,

another superstructure was analysed in Figure 3(e), whose repeated unit can be noted as $\bar{F}2\bar{F}3F3\bar{F}3F2F3(\bar{F}2)_7$, or $(40H)(F2)_7$, with translation of \bar{s}_3 . This structure can be determined as 246R with a space group of $R3m$ and an expression of $[F2F3\bar{F}2\bar{F}3F3\bar{F}3(F2)_7]_3$.

The expressions and crystallographic parameters of new polytypes of LPSO structures in this $Mg_{97}Zn_1Y_2$ alloy are summarised in Table 2. Further, the structural relationship between 18R, 14H and newly characterised LPSO structures in $Mg_{97}Zn_1Y_2$ alloy is outlined in Figure 4. Obviously, there exists a structure similarity between 60R and 78R structures, as both of them can be expressed as $(F2)_mF3\bar{F}3$ ($m = 1$ and 2) with a point group $\bar{3}m$, whilst the 14H, 26H and 38H structures can be presented as $(F2)_nF3(\bar{F}2)_n\bar{F}3$ ($n = 0, 1$ and 2) with a space group of $P6_3/mmc$. Moreover, some complex structures, such as 96R, 40H, 108H and 246R, are composed of simpler structures. In detail, they can be expressed as 96R, $(F2, 26H)_3$; 40H, $(26H, 14H)$; 108H, $(40H)_2(14H)_2$; 246R, $[(40H)(F2)_7]_3$. All these new structures consist of structure components of 18R and 14H structures, namely, F-blocks, 2-Mg and 3-Mg.

The size, morphology and volume of LPSO structures have been documented to play key roles in the mechanical properties of Mg–Zn–Y alloys [6,23]. LPSO structures, deformation kink of LPSO structures, and coherent interface between LPSO and Mg phase, are beneficial to strengthening and toughening Mg–Zn–Y alloys [6]. Further, recent investigations suggest that 18R-, 14H- and 10H- LPSO structures exhibit similar deformation behaviour at room temperature, but different slightly at high temperatures [24–26]. The stacking sequence of the LPSO structures and in-plane chemical ordering of Zn/Y atoms are proposed to affect the critical resolved shear stress (CRSS) of non-basal slips, and the macroscopic yield stress of 18R-, 14H- and 10H- LPSO structures. Tane et al. [27] indicated that the Zn/Y-enriched atomic layers, containing stable short-range ordered clusters, exhibit a high elastic modulus and contribute to the enhancement of the elastic modulus of the LPSO phase in the Mg alloys via first-principles calculations and micromechanics modelling. This result may imply that other parameters of LPSO structures, stacking period and building block (AB'CA or AB'C) [11,13,14], may also influence the mechanical properties of LPSO structures and those of Mg alloys. It is really challenging to study the effect of single LPSO phase on deformation behaviour and mechanical performance owing to the common intergrowth of LPSO phases [15,19]. Further quantitative analysis, the effect of stacking sequence, chemical distribution, and building blocks of LPSO structures on mechanical properties, are necessary for optimising the microstructure and will be systematically investigated in the future.

In summary, eight new polytypes of LPSO structures in a near-equilibrium $Mg_{97}Zn_1Y_2$ alloy, 60R, 78R, 26H, 96R, 38H, 40H, 108H and 246R, were characterised via a combination of TEM and Cs-corrected HAADF-STEM imaging at the atomic level. All of them are composed of F-blocks, 2-Mg and 3-Mg structure components. Their lattice parameter is derived as: $a_{LPSO} = a_{Mg} = 0.321\text{nm}$ and $c_{LPSO} = \frac{1}{2}n \times c_{Mg}$ ($n = \text{integer}$, corresponding to 60, 78, 26, 96, 38, 40, 108 and 246, respectively). The Bravais lattices and corresponding space groups are also deduced based on the introduced method.

Acknowledgements

We are also grateful to Prof. S. J. Zheng and Dr. Y. T. Zhou for fruitful discussion, Mr. B. Wu and Mr. L.X. Yang of this laboratory for their technical support on the Titan platform of the Titan^{3TM} G² 60-300kV aberration-corrected scanning transmission electron microscope.

Disclosure statement

No potential conflict of interest was reported by the authors.

Funding

This work was supported by the National Science Foundation of China [grant number 51301177]; the Innovation Fund of IMR [SCJJ-2013-PY-08], [2015-PY08]; the Youth Fund of SYNLF fund [2015FP18].

References

- [1] A. Inoue, Y. Kawamura, M. Matsushita, K. Hayashi and J. Koike, *J. Mater. Res.* 16 (2001) p.1894.
- [2] Y. Kawamura, K. Hayashi, A. Inoue and T. Masumoto, *Mater. Trans.* 42 (2001) p.1171.
- [3] Y. Kawamura, T. Kasahara, S. Izumi and M. Yamasaki *Scr. Mater.* 55 (2006) p.453.
- [4] Y. Kawamura and M. Yamasaki, *Mater. Trans.* 48 (2007) p.2986.
- [5] T. Itoi, K. Takahashi, H. Moriyama and M. Hirohashi, *Scr. Mater.* 59 (2008) p.1155.
- [6] X.H. Shao, Z.Q. Yang and X.L. Ma, *Acta Mater.* 58 (2010) p.4760.
- [7] M. Matsuda, S. Ii, Y. Kawamura, Y. Ikuhara and M. Nishida, *Mater. Sci. Eng. A* 393 (2005) p.269.
- [8] H. Yokobayashi, K. Kishida, H. Inui, M. Yamasaki and Y. Kawamura, *Acta Mater.* 59 (2011) p.7287.
- [9] K. Kishida, H. Yokobayashi, H. Inui, M. Yamasaki and Y. Kawamura, *Intermetallics* 31 (2012) p.55.
- [10] K. Kishida, H. Yokobayashi and H. Inui, *Philos. Mag.* 93 (2013) p.2826.
- [11] S.-B. Mi and Q.-Q. Jin, *Scr. Mater.* 68 (2013) p.635.
- [12] M. Yamasaki, M. Matsushita, K. Hagihara, H. Izuno, E. Abe and Y. Kawamura, *Scr. Mater.* 78 (2014) p.13.
- [13] Q.Q. Jin, X.H. Shao, X.B. Hu, Z.Z. Peng and X.L. Ma, *Philos. Mag.* 97 (2017) p.1.
- [14] Q.Q. Jin, X.H. Shao, Z.Z. Peng, J.H. You, K.Q. Qiu and X.L. Ma, *J. Alloys Compd* 693 (2017) p.1035.
- [15] Y.M. Zhu, A.J. Morton and J.F. Nie, *Acta Mater.* 58 (2010) p.2936.
- [16] D. Egusa and E. Abe, *Acta Mater.* 60 (2012) p.166.
- [17] J.E. Saal and C. Wolverton, *Scr. Mater.* 67 (2012) p.798.
- [18] S.Y. Ma, L.M. Liu and S.Q. Wang, *Mater. Sci. Forum* 749 (2013) p.569.
- [19] X. Shao, H. Yang, J.T. De Hosson and X. Ma, *Microsc. Microanal.* 19 (2013) p.1575.
- [20] K. Kishida, K. Nagai, A. Matsumoto, A. Yasuhara and H. Inui, *Acta Mater.* 99 (2015) p.228.
- [21] Q.-Q. Jin, C.-F. Fang and S.-B. Mi, *J. Alloy. Compd.* 568 (2013) p.21.
- [22] E. Abe, A. Ono, T. Itoi, M. Yamasaki and Y. Kawamura, *Philos. Mag. Lett.* 91 (2011) p.690.
- [23] E. Oñorbe, G. Garcés, P. Pérez and P. Adeva, *J. Mater. Sci.* 47 (2012) p.1085.
- [24] K. Hagihara, N. Yokotani and Y. Umakoshi, *Intermetallics* 18 (2010) p.267.
- [25] K. Hagihara, Y. Sugino, Y. Fukusumi, Y. Umakoshi and T. Nakano, *Mater. Trans.* 52 (2011) p.1096.
- [26] K. Hagihara, T. Okamoto, H. Izuno, M. Yamasaki, M. Matsushita, T. Nakano and Y. Kawamura, *Acta Mater.* 109 (2016) p.90.
- [27] M. Tane, Y. Nagai, H. Kimizuka, K. Hagihara and Y. Kawamura, *Acta Mater.* 61 (2013) p.6338.